

Article

# Paraffin Pickering Emulsion Stabilized with Nano-SiO<sub>2</sub> Designed for Wood Impregnation

Runhao Liu <sup>1</sup>, Xinyao Liu <sup>1</sup>, Yuting Zhang <sup>1</sup>, Junjia Liu <sup>1</sup>, Chengxi Gong <sup>1</sup>, Youming Dong <sup>1,\*</sup> , Jianzhang Li <sup>2</sup>, Jingbo Shi <sup>1</sup> and Miao Wu <sup>3</sup>

<sup>1</sup> College of Materials Science and Engineering, Nanjing Forestry University, Nanjing 210037, China; 18675045909@163.com (R.L.); lxynjlydx123@163.com (X.L.); zyt7528@163.com (Y.Z.); ljnjlydx123@163.com (J.L.); gcxaly@163.com (C.G.); shijb@njfu.edu.cn (J.S.)

<sup>2</sup> MOE Key Laboratory of Wooden Material Science and Application, Beijing Forestry University, Beijing 100083, China; lijzh@bjfu.edu.cn

<sup>3</sup> National Engineering Laboratory for Pulp and Paper, China National Pulp and Paper Research Institute Co. Ltd., Beijing 100102, China; miaowu0425@hotmail.com

\* Correspondence: youming.dong@njfu.edu.cn

Received: 9 June 2020; Accepted: 29 June 2020; Published: 2 July 2020



**Abstract:** Wax impregnation is an effective approach to improve wood water resistance. However, melted waxes require special equipment and cannot penetrate deep enough into wood. Recently, wax emulsions show excellent efficiency in wood modification. In this study, paraffin Pickering emulsion stabilized by low dispersed SiO<sub>2</sub> nanospheres was used to impregnate poplar wood. The microstructure and storage stability of the emulsion were evaluated. The dimensional stability, water uptake, wettability, and thermal stability of treated wood were also investigated. After homogenization, a milk-white oil-in-water (O/W) paraffin Pickering emulsion stabilized by the nano-SiO<sub>2</sub> (diameter of ~76 nm) was formed and demonstrated excellent storage stability. Paraffin Pickering emulsion could penetrate into the wood structure. The emulsion-treated wood was endowed with a moderate anti-swelling efficiency (ASE), high water resistance, and low wettability. Moreover, the addition of nano-SiO<sub>2</sub> could improve the thermal stability of the treated wood.

**Keywords:** wood modification; wax impregnation; paraffin Pickering emulsion; nano-SiO<sub>2</sub>

## 1. Introduction

Wood, as a biomaterial, has been ubiquitously used in furniture, decoration, and constructions. Because of increased environmental awareness and better living standards, there is a growing demand for wood-based products [1]. However, wood is a hygroscopic material that is sensitive to water and biological attacks, resulting in dimensional instability and susceptibility, when subjected to fluctuating humidity and degradation by fungi [2].

Different methods, including chemical modifications [3,4], impregnation [5,6], and heat treatments [7], have been exploited to enhance the water resistance of wood. Among these methods, wax impregnation is commercially available and effective due to the high hydrophobicity of wax [8,9]. Esteves et al. impregnated *Pinus pinaster* Ait. wood with hot melting waxes using a hot-cold process and reported that the equilibrium moisture content decreased by 70% and dimensional stability (ASE) reached 16–71% at 65% relative humidity [10]. In addition, wax impregnation can reduce weathering and improve the termite resistance of wood [11,12]. However, melted waxes cannot penetrate deeper into the wood, and special equipment is required in the treatment process [13]. Compared with the melted waxes, wax emulsions exhibit better efficiency in the improvement of water resistance of wood [14]. For example, 2% wax emulsion was reported to increase the dimensional stability

and decrease the water absorption of treated wood significantly [15]. Wax emulsion is also useful in combination with other modification methods, such as heat and plasma treatment, and wood preservatives [16–18].

Generally, the wax emulsion is a dispersion in which the hydrophobic wax is homogeneously dispersed in water in the presence of emulsifiers. Recently, solid particles have been used to stabilize the interfaces, raising renewed interest in their extensive applications. Nano and micro solid particles can accumulate at the interface between two immiscible liquids and form a monolayer between the dispersed and continuous phases. The resultant emulsion is known as a Pickering emulsion [19]. Compared with conventional surfactants, particulate emulsifiers have many potential advantages, such as more robust and reproducible formulations, reduced foaming problems, lower toxicity profiles and cost [20]. Solid particles could be used to stabilize the paraffin emulsion for wood impregnation. Jiang et al. prepared the paraffin Pickering emulsion, synergistically stabilized by nano-SiO<sub>2</sub> and traditional surfactants [21]. They found that the incorporation of nano-SiO<sub>2</sub> improved emulsion stability and reduced the droplet size. In addition, the silica also had a beneficial effect on the hardness, mechanical properties, and thermal stability of wood. Various particles such as latex particles [22], Fe<sub>3</sub>O<sub>4</sub> [23], and organomontmorillonites [24] were studied to stabilize Pickering emulsions.

In this study, the low dispersion nano-SiO<sub>2</sub> was synthesized and used to stabilize paraffin Pickering emulsion. The stability and microstructure of the prepared paraffin Pickering emulsion were characterized. In addition, the properties of poplar wood impregnated with the paraffin Pickering emulsion were investigated.

## 2. Materials and Methods

### 2.1. Materials

Paraffin wax (a mixture of long alkanes with a melting temperature from 54–56 °C), tetraethyl orthosilicate (TEOS, 99%), and ammonium hydroxide solution (25–28% NH<sub>3</sub> in water) were purchased from Shanghai Macklin Biochemical Co., Ltd. (Shanghai, China). Wood sample boards were cut from the fast-growing poplar (*Populus tomentosa* Carr.) logs. The final sample size was 20 (tangential) × 20 (radial) × 10 (longitudinal) mm<sup>3</sup>, as shown in Figure 1. All samples were free of defects and the oven-dried density was 0.33 g/cm<sup>3</sup>. There were ten replicates in each group.

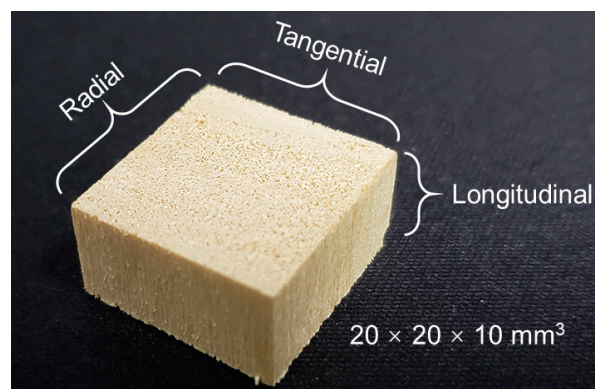


**Figure 1.** Photograph of a poplar sample. The sample size was 20 (tangential) × 20 (radial) × 10 (longitudinal) mm<sup>3</sup>.

### 2.2. Synthesis of Low Dispersed Nano SiO<sub>2</sub> Spheres

Nano-SiO<sub>2</sub> solid spheres were prepared using the Stöber process. TEOS (4 mL) and ethanol (100 mL) were sufficiently mixed and added to the mixture of water (4 mL), ethanol (100 mL), and ammonium hydroxide solution (8 mL) in a flask. The mixture was then magnetically stirred (400 rpm) for 6 h at room temperature. Afterwards, the mixture was centrifuged (10,000 rpm, 20 min) twice, and

the supernatant was then decanted and dispersed in fresh water. The resulting particles were dried into powders.

### 2.3. Preparation of Paraffin Pickering Emulsion

Paraffin Pickering emulsion was prepared as follows: First, nano-SiO<sub>2</sub> and water (2% by weight) were mixed by an ultrasonic processor (Sonics VCX 800, Newtown, CT, USA) for 30 min. Second, the paraffin wax (10% by weight) was added to the aqueous dispersion and heated at 70 °C to melt the wax. Finally, the resultant was homogenized by an Ultra Turrax T18 homogenizer (IKA, Staufen, Germany) for 5 min under 12,000 rpm.

### 2.4. Wood Impregnation with Paraffin Pickering Emulsion

Wood samples were impregnated with the paraffin Pickering emulsion (950 mbar for 30 min and atmospheric pressure for 6 h). After impregnation, the wood samples were placed into an oven to redistribute the paraffin wax within the wood for 10 h at 100 °C, followed by being oven-dried at 103 °C to a constant mass.

### 2.5. Characterization of the Monodisperse SiO<sub>2</sub> Spheres and Paraffin Pickering Emulsion

The microstructure of the SiO<sub>2</sub> nanospheres was observed by a Quanta FEG 250 scanning electron microscopy (SEM, FEI Corporate, Hillsboro, OR, USA) with 5 kV and a JEOL 2100F transmission electron microscopy (TEM, Tokyo, Japan) with 200 kV. The droplet morphology of emulsions was observed by an optical microscopy (Leica DM2500, Wetzlar, Germany).

### 2.6. Characterization of the Modified Wood

The morphology of untreated and emulsion treated wood samples was characterized by a SEM (Quanta FEG 250, FEI Corporate, Hillsboro, OR, USA) with 5 kV. In addition, The C and Si elements in the treated wood sample were detected by an energy-dispersive spectrometer (EDS).

The untreated and treated wood samples were analyzed using Nicolet iS50 Fourier-transform infrared spectrophotometer (FTIR, Thermo Fisher Scientific, Madison, WI, USA) equipped with an ATR accessory from 4000 to 400 cm<sup>-1</sup> with the 4 cm<sup>-1</sup> resolution for 32 scans.

The weight percent gain (WPG) of the emulsion treated wood sample was calculated as follows:

$$WPG (\%) = (W_2 - W_1) / W_1 \times 100 \quad (1)$$

where  $W_1$  and  $W_2$  are the oven-dried weights of wood samples before and after the treatment, respectively.

Both untreated and treated wood samples were immersed in deionized water. The weight and dimensions were taken after different immersion times (6, 24, 48, 72, and 120 h). Water uptake (WU) was calculated as follows:

$$WU (\%) = (W_3 - W_2) / W_2 \times 100 \quad (2)$$

where  $W_3$  is the weight of wood sample after immersion.

The anti-swelling efficiency (ASE) after 72 h immersion was used to assess the dimensional stability of wood and calculated based on the swelling difference between the untreated and treated wood samples:

$$ASE (\%) = (S_u - S_t) / S_u \times 100 \quad (3)$$

where  $S_u$  and  $S_t$  were volumetric swelling of the untreated and treated wood samples, respectively.

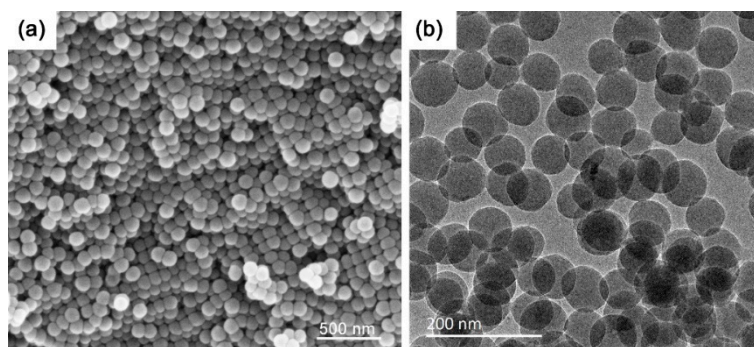
Wettability on the tangential surfaces of wood samples was tested by a contact angle goniometer (DSA100, Krüss GmbH, Hamburg, Germany): 3 µL droplets of deionized water were placed on the wood surface using a micro-syringe, from which the average angles of the drops were collected for a total duration of 120 s.

Thermogravimetric analysis was conducted by a TGA55 analyzer (TA Instruments, New Castle, DE, USA) with a heating rate of 10 °C/min from room temperature to 600 °C in nitrogen atmosphere.

### 3. Results and Discussion

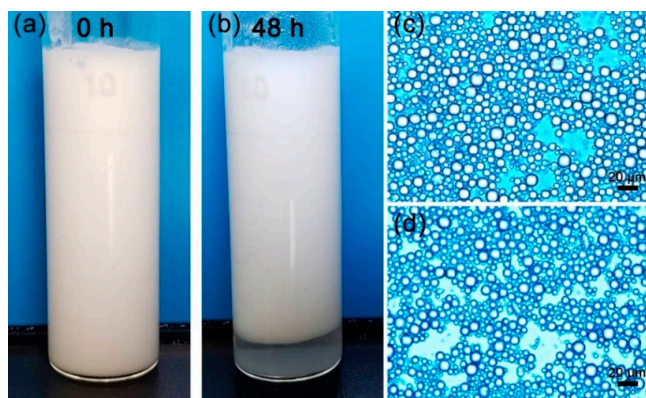
#### 3.1. Analysis of the Paraffin Pickering Emulsion

Figure 2 shows the typical SEM and TEM images of the obtained SiO<sub>2</sub> solid spheres, which indicated that the ~76 nm SiO<sub>2</sub> nanospheres were spherical and showed a low level of dispersal. The surface of the nanospheres was clean and no obvious conglutination or agglomeration can be observed.



**Figure 2.** Microstructure of SiO<sub>2</sub> nanospheres: (a) SEM image and (b) TEM image. The average size in diameter was ~76 nm.

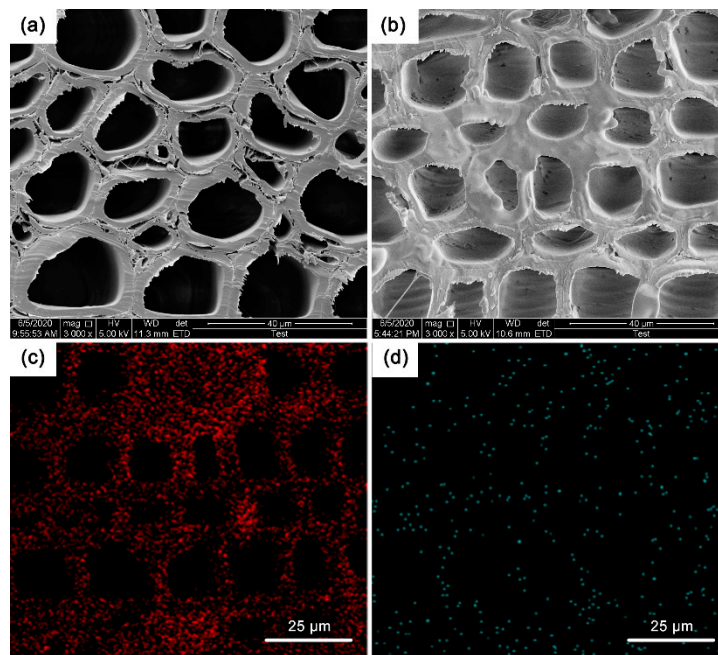
A drop of the prepared paraffin Pickering emulsion could disperse readily in the deionized water, indicating an oil-in-water (O/W) emulsion. The appearance of the paraffin Pickering emulsion stabilized by SiO<sub>2</sub> nanospheres is presented in Figure 3a. After homogenization, a milk-white Pickering emulsion was formed. The emulsion droplets shown in Figure 3c, are spherical, with diameters of ~8 μm. As shown in Figure 3b, no pure wax layer was released from the emulsion after 48 h storage, but water separation was observed. This was because the emulsion was micro-sized, and the lighter oil droplets tended to float [25]. The size of the droplets remained unchanged after 48 h storage, indicating excellent storage stability. A previous study reported that stable emulsion cannot be obtained by SiO<sub>2</sub> alone [21]. However, the wax they used was liquid paraffin wax, which may coalesce easily during the emulsion storage. On the contrary, the droplets formed by solid paraffin wax can coagulate at room temperature and separate in water due to the effect of nano-SiO<sub>2</sub> embed in the surface of solid droplets.



**Figure 3.** Photographs of the paraffin Pickering emulsion stabilized by the SiO<sub>2</sub> nanospheres. (a,b) were photographed after 0 h and 48 h storage, respectively. (c,d) were the corresponding optical microscopy images of (a,b), respectively. The size of the droplets remained unchanged after 48-h storage, indicating an excellent storage stability of the prepared emulsion.

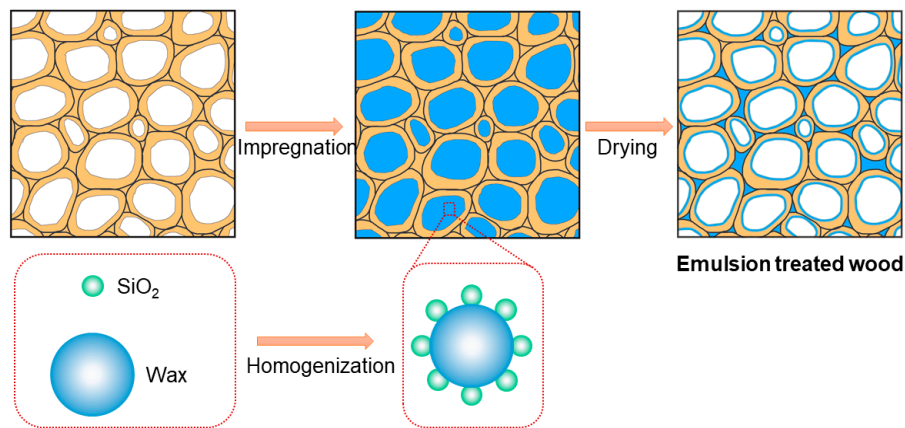
### 3.2. Microstructure and Chemical Analysis of the Emulsion Treated Wood

Figure 4 displays the microstructure of transverse sections for untreated and emulsion treated wood samples. The empty cell lumens and cell wall structure of untreated wood samples, such as the middle lamella and cell corners are clearly demonstrated in Figure 4a. After impregnation, a layer of waxy substrate was deposited on the cell lumen walls, as seen in Figure 4b. The middle lamella and cell corners of wood were also filled with wax, indicating the wax could penetrate into these tissues. Wang et al. pointed out that wax can adhere to the interior wood surfaces after de-emulsification and thus improve the water resistance [16]. Additionally, the EDS images, shown in Figure 4c,d, demonstrate that more Si element appeared in the wood structure, indicating penetration of SiO<sub>2</sub> into the wood structure along with the wax. During the drying process, the wax was redistributed in the wood structure, and part of the SiO<sub>2</sub> spheres was released from the emulsion and adhered to the interior wood surfaces. Figure 5 illustrates the fabrication process of the emulsion treated wood. The paraffin Pickering emulsion stabilized by SiO<sub>2</sub> penetrated into the wood structure through the impregnation. During drying, water was released and the emulsion was de-emulsified. Most of the wax and SiO<sub>2</sub> could adhere to the interior wood surface and infiltrate into the middle lamella and cell corners of the wood.



**Figure 4.** Morphologies of (a) untreated and (b) emulsion treated wood samples. (c,d) were the C element distribution and Si element distribution images of treated sample, respectively. After impregnation, the cell lumen walls were covered by a layer of waxy substrate, and the middle lamella and cell corners of wood were also filled with wax. The distribution of Si element in wood structure indicated the SiO<sub>2</sub> penetrated into wood along with the wax.

The FTIR spectra of SiO<sub>2</sub>, wax, untreated, and treated wood samples are displayed in Figure 6. In the spectrum of wax, the absorption peaks at 2916 and 2848 cm<sup>-1</sup> were attributed to the symmetrical and asymmetrical stretching of C-H in CH<sub>2</sub> and CH<sub>3</sub>, respectively [26]. The peaks at 1462 and 720 cm<sup>-1</sup> were due to the bending vibration and rocking vibration of CH<sub>2</sub>, respectively [27]. The main absorption peak in the SiO<sub>2</sub> spectrum at 1104 cm<sup>-1</sup> was related to the asymmetric stretching of Si-O-Si [28]. Peaks at 2916, 2848, and 720 cm<sup>-1</sup>, which appeared in the spectrum of treated wood samples, were new, and the intensity of peaks at 1462 and 1104 cm<sup>-1</sup> was enhanced. These results indicate the successful penetration of the paraffin Pickering emulsion into the wood structure.



**Figure 5.** Illustration of the fabrication process of the emulsion treated wood. After drying, the paraffin Pickering emulsion was de-emulsified and adhered to the interior wood surfaces.

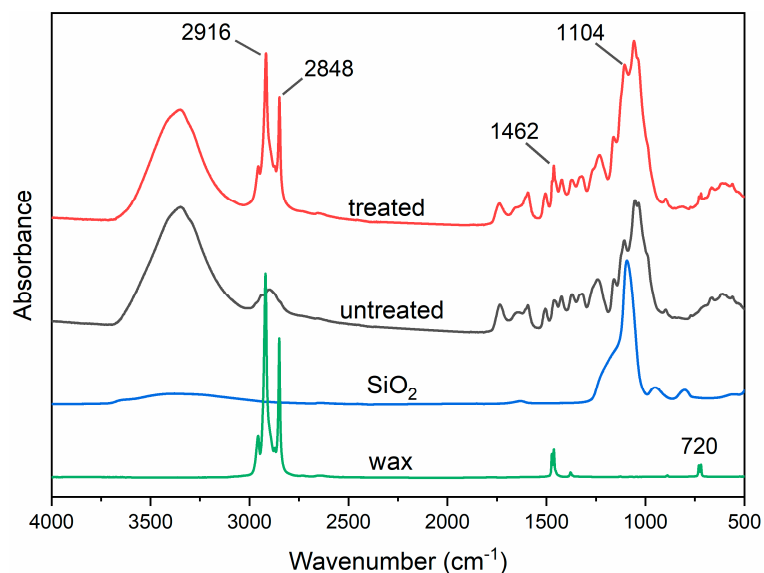


**Figure 6.** Fourier-transform infrared spectrophotometer (FTIR) spectra of the SiO<sub>2</sub>, wax, untreated, and treated wood samples. Due to the impregnation, new peaks at 2916, 2848, and 720 cm<sup>-1</sup>, derived from wax, appeared in the spectrum of treated wood samples and the peaks at 1462 and 1104 cm<sup>-1</sup> were also enhanced.

### 3.3. Properties of the Emulsion Treated Wood

Figure 7a displays the WPG and ASE of wood samples impregnated with paraffin Pickering emulsion. The WPG value of the treated wood sample was 8.7%, which endowed the wood with an ASE of 19%. Esteves et al. used hot melting wax to impregnate pine wood, and found that the ASE at 65% relative humidity reached 41% and 61% in radial and tangential directions, respectively [10]. Wang et al. [29] reported that 4.89% WPG was obtained by 2% wax emulsion impregnation and the swelling rate was significantly decreased. The water uptake of the emulsion treated samples as a function of time is shown in Figure 7b. With the prolonged immersion time, the water uptake was improved for both untreated and treated samples, due to water filling of the capillaries and void spaces in the wood structure. The water uptake increased more quickly during the initial 24 h than the subsequent period. After 144 h immersion, the water uptake of untreated wood samples was 114%, while that of the treated samples was 90%. The water uptake of treated wood samples decreased by 21% compared with the untreated one. This efficient waterproof property of wax impregnation was

also reported in the previous studies [14,21,30,31]. Paraffin Pickering emulsion could penetrate into the wood structure and form a hydrophobic layer after drying, which restricts the intrusion of water.

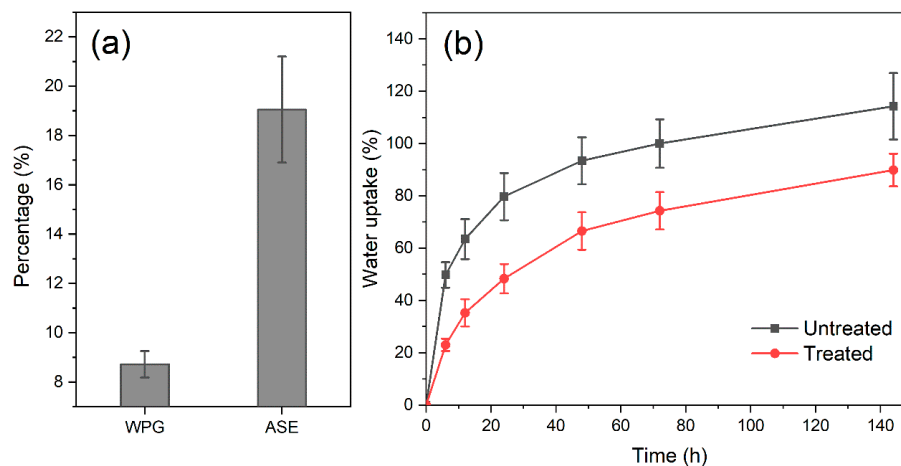


**Figure 7.** (a) Weight percent gain (WPG) and anti-swelling efficiency (ASE) of the treated wood sample, (b) water uptake of untreated and treated wood sample as a function of time. The ASE of treated wood sample reached 19% at WPG of 8.7%.

Figure 8 shows the dynamic wettability of both untreated and treated wood samples. All samples were planed by 1–2 mm before the measurement to reduce the influence of residues of modifiers and the surface aging. For untreated wood samples, the contact angles decreased rapidly in the initial 10 s, after which the contact angles decreased slowly until the droplet completely penetrated the wood surface. Compared with untreated wood samples, treated ones exhibited higher initial contact angle ( $124^\circ$  vs.  $101^\circ$ ) with succeeding measurements maintained above  $110^\circ$ , which was in fair agreement with Jiang's study [21]. The increased angle could be due to the blocking of the wood structure and the high hydrophobicity of the paraffin wax in the structure.

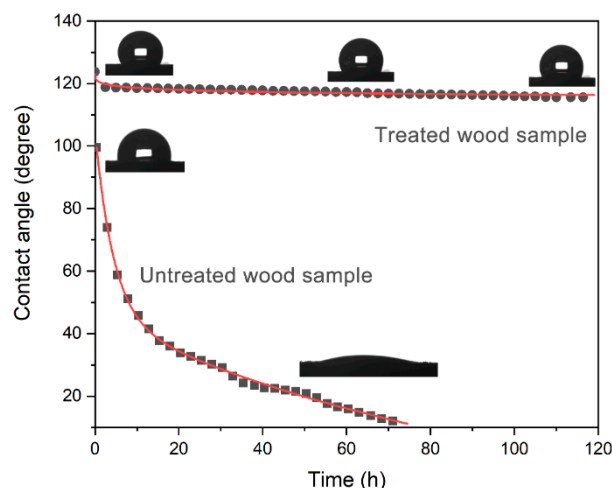


**Figure 8.** Dynamic wettability of both untreated and treated wood samples. The treated wood sample exhibited higher initial contact angle than untreated wood, and the succeeding measurements maintained above  $110^\circ$ .

In addition to serving as a solid surfactant, the incorporation of nano-SiO<sub>2</sub> could improve the thermal stability of wood because of the inorganic nature of SiO<sub>2</sub>. Therefore, the thermal stability of untreated and emulsion treated wood samples was analyzed using TGA. Figure 9 displays the thermogravimetric (TG) and differential thermogravimetric (dTG) curves of the samples. For untreated wood, the first degradation region from 30 to 120 °C was related to the release of free and bound water

from the wood [32]. The most degradation actions occurred between 160 and 400 °C, at which the hemicellulose and cellulose were significantly degraded and the maximum decomposition temperature was 345 °C (dTG curve). At finish, the weight residue of the untreated wood was about 12%. For emulsion treated sample, an obvious weight loss (~10%) between 120 and 230 °C appeared, which could be due to the degradation of paraffin wax [33]. The maximum decomposition temperature was decreased to 327 °C (dTG curve). However, the weight residue after the thermal degradation was 16%, which could be due to the enhancement of nano-SiO<sub>2</sub> for the char structure [34].

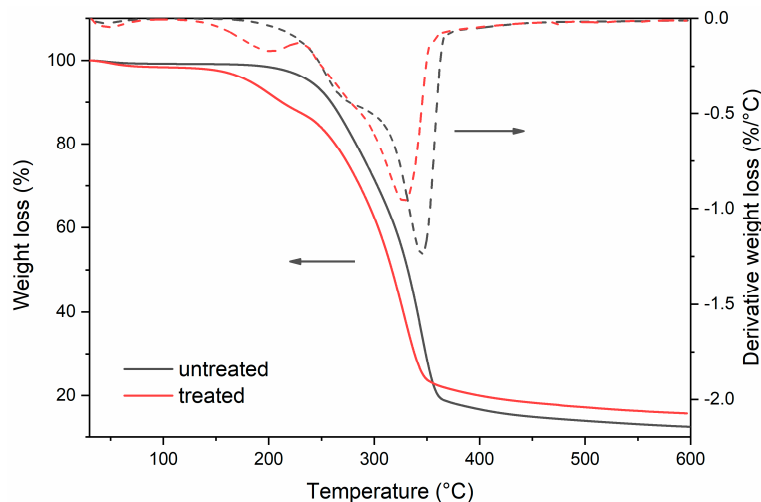


**Figure 9.** Thermogravimetric (TG) and differential thermogravimetric (dTG) curves of untreated and treated wood samples. The treated wood sample had higher weight residue than untreated wood.

#### 4. Conclusions

The low dispersed SiO<sub>2</sub> nanospheres were synthesized with the diameter ~76 nm, and these nanospheres were effective in stabilizing the paraffin Pickering emulsion. Due to the filling of wax and SiO<sub>2</sub> nanospheres, the impregnation with emulsion could endow wood with moderate ASE, high water resistance, and low wettability. The thermal stability of wood was also improved due to the presence of nano-SiO<sub>2</sub>. This preliminary investigation provides a promising method to enhance the dimensional and thermal stability of wood. However, more efforts are needed in the future to investigate the effects of many treatment variables, such as particle content, particle size, surface polarity, and the emulsion process, on the properties of emulsions and impregnated wood.

**Author Contributions:** Methodology and data curation, R.L., X.L., Y.Z., C.G., J.L. (Junjia Liu) and M.W.; writing—original draft preparation, R.L. and X.L.; supervision, Y.D.; writing—review and editing, Y.D., J.S. and J.L. (Jianzhang Li); project administration and funding acquisition, Y.D. All authors have read and agreed to the published version of the manuscript.

**Funding:** This research was funded by Natural Science Foundation of Jiangsu Province, grant number BK20190754, and Student Practice Innovation and Training Program of Jiangsu Province, grant number 201910298001Z.

**Conflicts of Interest:** The authors declare no conflict of interest.

#### References

1. Militz, H.; Lande, S. Challenges in wood modification technology on the way to practical applications. *Wood Mater. Sci. Eng.* **2009**, *4*, 23–29. [[CrossRef](#)]
2. Altgen, M.; Awais, M.; Altgen, D.; Klüppel, A.; Mäkelä, M.; Rautkari, L. Distribution and curing reactions of melamine formaldehyde resin in cells of impregnation-modified wood. *Sci. Rep.* **2020**, *10*, 1–10. [[CrossRef](#)] [[PubMed](#)]

3. Dong, Y.; Wang, K.; Yan, Y.; Zhang, S.; Li, J. Grafting polyethylene glycol dicrylate (PEGDA) to cell walls of poplar wood in two steps for improving dimensional stability and durability of the wood polymer composite. *Holzforschung* **2016**, *70*, 919–926. [[CrossRef](#)]
4. Li, J.; Furuno, T.; Zhou, W.-R.; Ren, Q.; Han, X.-Z.; Zhao, J.-P. Properties of acetylated wood prepared at low temperature in the presence of catalysts. *J. Wood Chem. Technol.* **2009**, *29*, 241–250. [[CrossRef](#)]
5. Dong, Y.; Yan, Y.; Wang, K.; Li, J.; Zhang, S.; Xia, C.; Shi, S.Q.; Cai, L. Improvement of water resistance, dimensional stability, and mechanical properties of poplar wood by rosin impregnation. *Eur. J. Wood Prod.* **2015**, *74*, 177–184. [[CrossRef](#)]
6. Qin, Y.; Dong, Y.; Li, J. Effect of modification with melamine–urea–formaldehyde resin on the properties of eucalyptus and poplar. *J. Wood Chem. Technol.* **2019**, *39*, 360–371. [[CrossRef](#)]
7. Altgen, D.; Altgen, M.; Kyyrö, S.; Rautkari, L.; Mai, C. Time-dependent wettability changes on plasma-treated surfaces of unmodified and thermally modified European beech wood. *Eur. J. Wood Prod.* **2020**, *78*, 417–420. [[CrossRef](#)]
8. Wang, W.; Huang, Y.; Cao, J.; Zhu, Y. Penetration and distribution of paraffin wax in wood of loblolly pine and Scots pine studied by time domain NMR spectroscopy. *Holzforschung* **2018**, *72*, 125–131. [[CrossRef](#)]
9. Dong, Y.; Wang, K.; Li, J.; Zhang, S.; Shi, S.Q. Environmentally benign wood modifications: A review. *ACS Sustain. Chem. Eng.* **2020**, *8*, 3532–3540. [[CrossRef](#)]
10. Esteves, B.; Nunes, L.; Domingos, I.; Pereira, H. Improvement of termite resistance, dimensional stability and mechanical properties of pine wood by paraffin impregnation. *Eur. J. Wood Prod.* **2014**, *72*, 609–615. [[CrossRef](#)]
11. Lesar, B.; Pavlič, M.; Petrič, M.; Škapin, A.S.; Humar, M. Wax treatment of wood slows photodegradation. *Polym. Degrad. Stab.* **2011**, *96*, 1271–1278. [[CrossRef](#)]
12. Scholz, G.; Militz, H.; Gascón-Garrido, P.; Ibiza-Palacios, M.; Oliver-Villanueva, J.-V.; Peters, B.; Fitzgerald, C. Improved termite resistance of wood by wax impregnation. *Int. Biodeterior. Biodegrad.* **2010**, *64*, 688–693. [[CrossRef](#)]
13. Scholz, G.; Krause, A.; Militz, H. Capillary water uptake and mechanical properties of wax soaked Scots pine. In Proceedings of the Fourth European Conference on Wood Modification, Stockholm, Sweden, 27–29 April 2009; Englund, F., Hill, C.A.S., Militz, H., Segerholm, B.K., Eds.; SP Technical Research Institute of Sweden: Stockholm, Sweden, 2009.
14. Lesar, B.; Humar, M. Use of wax emulsions for improvement of wood durability and sorption properties. *Eur. J. Wood Prod.* **2010**, *69*, 231–238. [[CrossRef](#)]
15. Chau, T.; Ma, E.; Yang, T. Moisture sorption and hygroexpansion of paraffin wax emulsion-treated Southern pine (*Pinus* spp.) under dynamic conditions. *For. Prod. J.* **2017**, *67*, 463–470. [[CrossRef](#)]
16. Wang, W.; Zhu, Y.; Cao, J.; Guo, X. Thermal modification of Southern pine combined with wax emulsion preimpregnation: Effect on hydrophobicity and dimensional stability. *Holzforschung* **2015**, *69*, 405–413. [[CrossRef](#)]
17. Avramidis, G.; Scholz, G.; Nothnick, E.; Militz, H.; Viöl, W.; Wolkenhauer, A. Improved bondability of wax-treated wood following plasma treatment. *Wood Sci. Technol.* **2010**, *45*, 359–368. [[CrossRef](#)]
18. Liu, M.; Zhong, H.; Ma, E.; Liu, R. Resistance to fungal decay of paraffin wax emulsion/copper azole compound system treated wood. *Int. Biodeterior. Biodegrad.* **2018**, *129*, 61–66. [[CrossRef](#)]
19. Kaewsaneha, C.; Tangboriboonrat, P.; Polpanich, D.; Eissa, M.; Elaissari, A. Preparation of Janus colloidal particles via Pickering emulsion: An overview. *Colloids Surf. A Physicochem. Eng. Asp.* **2013**, *439*, 35–42. [[CrossRef](#)]
20. Fujii, S.; Read, E.S.; Binks, B.P.; Armes, S.P. Stimulus-responsive emulsifiers based on nanocomposite microgel particles. *Adv. Mater.* **2005**, *17*, 1014–1018. [[CrossRef](#)]
21. Jiang, J.; Cao, J.; Wang, W.; Shen, H. Preparation of a synergistically stabilized oil-in-water paraffin Pickering emulsion for potential application in wood treatment. *Holzforschung* **2018**, *72*, 489–497. [[CrossRef](#)]
22. Vasantha, V.A.; Hua, N.Q.; Rusli, W.; Hadia, N.J.; Stubbs, L.P. Unique oil-in-brine Pickering emulsion using responsive antipolyelectrolyte functionalized latex: A versatile emulsion stabilizer. *ACS Appl. Mater. Interfaces* **2020**, *12*, 23443–23452. [[CrossRef](#)]
23. Lin, Z.; Zhang, Z.; Li, Y.; Deng, Y. Magnetic nano-Fe<sub>3</sub>O<sub>4</sub> stabilized Pickering emulsion liquid membrane for selective extraction and separation. *Chem. Eng. J.* **2016**, *288*, 305–311. [[CrossRef](#)]

24. Zhou, D.; Zhang, Z.; Tang, J.; Zhao, J.; Liao, L. Effect of emulsification processes on the stability of Pickering emulsions stabilized by organomontmorillonites. *J. Dispers. Sci. Technol.* **2016**, *38*, 1030–1034. [[CrossRef](#)]
25. Low, L.E.; Tey, B.T.; Ong, B.H.; Chan, E.-S.; Tang, S.Y. Palm olein-in-water Pickering emulsion stabilized by Fe<sub>3</sub>O<sub>4</sub>-cellulose nanocrystal nanocomposites and their responses to pH. *Carbohydr. Polym.* **2017**, *155*, 391–399. [[CrossRef](#)]
26. Fang, Y.; Wei, H.; Liang, X.; Wang, S.; Liu, X.; Gao, X.; Zhang, Z. Preparation and thermal performance of silica/n-tetradecane microencapsulated phase change material for cold energy storage. *Energy Fuels* **2016**, *30*, 9652–9657. [[CrossRef](#)]
27. Zhang, Y.; Li, W.; Huang, J.; Cao, M.; Du, G. Expanded graphite/paraffin/silicone rubber as high temperature form-stabilized phase change materials for thermal energy storage and thermal interface materials. *Mater.* **2020**, *13*, 894. [[CrossRef](#)]
28. Zhang, N.; Li, Z.; Xiao, Y.; Pan, Z.; Jia, P.; Feng, G.; Bao, C.; Zhou, Y.; Hua, L. Lignin-based phenolic resin modified with whisker silicon and its application. *J. Bioresour. Bioprod.* **2020**, *5*, 69–77. [[CrossRef](#)]
29. Wang, J.; Zhong, H.; Ma, E.; Cao, J. Properties of wood treated with compound systems of paraffin wax emulsion and copper azole. *Eur. J. Wood Prod.* **2016**, *76*, 315–323. [[CrossRef](#)]
30. Chen, C.; Chen, J.; Zhang, S.; Cao, J.; Wang, W. Forming textured hydrophobic surface coatings via mixed wax emulsion impregnation and drying of poplar wood. *Wood Sci. Technol.* **2020**, *54*, 421–439. [[CrossRef](#)]
31. Reinprecht, L.; Repák, M. The Impact of paraffin-thermal modification of beech wood on its biological, physical and mechanical properties. *Forests* **2019**, *10*, 1102. [[CrossRef](#)]
32. Dong, Y.; Yan, Y.; Zhang, S.; Li, J. Wood/polymer nanocomposites prepared by impregnation with furfuryl alcohol and nano-SiO<sub>2</sub>. *BioResources* **2014**, *9*, 6028–6040. [[CrossRef](#)]
33. Guo, X.; Zhang, L.; Cao, J.; Peng, Y. Paraffin/wood flour/high-density polyethylene composites for thermal energy storage material in buildings: A morphology, thermal performance, and mechanical property study. *Polym. Compos.* **2017**, *39*, E1643–E1652. [[CrossRef](#)]
34. Liu, X.; Chen, X.; Ren, J.; Chang, M.; He, B.; Zhang, C. Effects of nano-ZnO and nano-SiO<sub>2</sub> particles on properties of PVA/xylan composite films. *Int. J. Boil. Macromol.* **2019**, *132*, 978–986. [[CrossRef](#)] [[PubMed](#)]



© 2020 by the authors. Licensee MDPI, Basel, Switzerland. This article is an open access article distributed under the terms and conditions of the Creative Commons Attribution (CC BY) license (<http://creativecommons.org/licenses/by/4.0/>).